

Published in final edited form as:

Breast Cancer Res Treat. 2014 November ; 148(2): 291–302. doi:10.1007/s10549-014-3164-7.

Emodin suppresses pulmonary metastasis of breast cancer cells accompanied with decreased macrophage recruitment and M2 polarization in the lungs

Xuemei Jia^{1,2}, Fang Yu^{2,3}, Junfeng Wang^{2,4}, Stephen Iwanowycz², Fatma Saaoud², Yuzhen Wang², Jun Hu⁵, Qian Wang⁵, and Daping Fan^{2,*}

¹Department of Gynecology, the First Affiliated Hospital of Nanjing Medical University, Nanjing, 210029, China

²Department of Cell Biology and Anatomy, University of South Carolina School of Medicine, Columbia, SC 29209

³Department of Nutrition and Food Hygiene, Fourth Military Medical University, Xi'an, 710032, China

⁴Centre for Stem Cell Research and Application, Union Hospital, Tongji Medical College, Huazhong University of Science and Technology, Wuhan, 430022, China

⁵Department of Chemistry and Biochemistry, University of South Carolina, Columbia, SC 29208

Abstract

Purpose—Breast cancer is the leading cause of death in female cancer patients due to the lack of effective treatment for metastasis. Macrophages are the most abundant immune cells in the primary and metastatic tumors, and contribute to tumor initiation, progression and metastasis. Emodin has been found to exert anti-tumor effects through promoting cell cycle arrest and apoptosis, and inhibiting angiogenesis, but its effects on tumor-associated macrophages during cancer metastasis have not been investigated.

Methods—Mice inoculated with 4T1 or EO771 breast cancer cells orthotopically were treated with Emodin after the primary tumors reached 200 mm³ in size. Primary tumor growth, lung metastasis, and macrophage infiltration in the lungs were analyzed. *In vitro* experiments were performed to examine the effects of Emodin on macrophage migration and M2 polarization, and the underlying mechanisms.

Results—Emodin significantly suppressed breast cancer lung metastasis in both orthotopic mouse models without apparent effects on primary tumors. Reduced infiltration of F4/80+ macrophages and Ym1+ M2 macrophages in lungs was observed in Emodin-treated mice. *In vitro* experiments demonstrated that Emodin decreased the migration of macrophages towards tumor cell conditioned medium (TCM) and inhibited macrophage M2 polarization induced by TCM.

*Correspondence: Daping Fan, Department of Cell Biology and Anatomy, University of South Carolina School of Medicine, 6439 Garners Ferry Road, Columbia, SC 29208. Phone: 803-216-3806; Fax: 803-216-3846; daping.fan@uscmed.sc.edu.

Disclosure of Potential Conflicts of Interest

No potential conflicts of interest were disclosed.

Mechanistically, Emodin suppressed STAT6 phosphorylation and C/EBP β expression, two crucial signaling events in macrophage M2 polarization, in macrophages treated with IL-4 or TCM.

Conclusion—Taken together, our study, for the first time, demonstrated that Emodin suppressed pulmonary metastasis of breast cancer probably through inhibiting macrophage recruitment and M2 polarization in the lungs by reducing STAT6 phosphorylation and C/EBP β expression.

Keywords

Emodin; breast cancer; pulmonary metastasis; macrophage; polarization

Introduction

Breast cancer is the leading cause of cancer-related death among women worldwide [1]. Although comprehensive treatments such as anti-angiogenic or hormonal therapies combined with other agents have been developed to treat breast cancer [2], 90% of patients do not survive metastatic tumors in organs such as lung, bone, brain or liver [3, 4]. New therapeutic strategies are urgently needed.

Macrophages are the most abundant immune cells in tumor microenvironment [5]. Both clinical and experimental studies have shown that tumor-associated macrophages (TAM) promote tumor growth and progression through extracellular matrix remodeling, promotion of tumor cell migration and invasion, angiogenesis, and immune suppression [5–8]. Stromal and tumor cell derived chemokines and growth factors recruit circulating monocytes and facilitate their differentiation into macrophages in primary tumors of a variety of cancers, including breast cancer [9, 10]. In addition to their well-characterized functions in primary tumors, macrophages have been shown to play important roles in metastatic sites [11–17]. Recent *ex vivo* imaging studies have shown that macrophages were recruited towards extravasating tumor cells, and that depletion of these macrophages dramatically reduced the seeding, extravasation, and the subsequent survival of tumor cells [13]. Another study showed that metastasis-associated macrophages (MAMs) provided survival and growth signals to metastatic tumor cells through binding of $\alpha 4$ -integrin to VCAM-1 on tumor cells [14]. Although increasing evidences have demonstrated the critical roles of macrophages in tumor metastasis, molecular mechanisms responsible for their differentiation, accumulation and tumor-promoting functions warrant further investigation. Strategies to block the recruitment and function of MAMs are of conceivable therapeutic value.

Emodin (1,3,8-trihydroxy-6-methylanthraquinone) is a natural anthraquinone derivative isolated from *Rheum palmatum L* and some other Chinese herbs [18]. It has been shown to have anti-atherogenic, anti-inflammatory, as well as anti-cancer effects [19–21]. As a pleiotropic molecule, Emodin affects the expression of several critical inflammatory factors including NF- κ B, TNF α , iNOS, IL-10, and CXCR4 [22], indicating its potential therapeutic value in inflammatory diseases. Recent studies have shown that Emodin suppresses the growth of various cancers through inducing cell cycle arrest, promoting apoptosis, or inhibiting angiogenesis [21–25]. However, if and how Emodin exerts anti-tumor effects through modulating inflammatory microenvironment or acting on immune cells has not been reported.

Our study, for the first time, demonstrated that Emodin inhibited pulmonary metastasis in 4T1 and EO771 orthotopic breast cancer mouse models through inhibiting macrophage recruitment and M2 polarization in metastatic lungs via suppressing STAT6 phosphorylation and C/EBP β expression. Our data suggest that Emodin used alone or in combination with conventional treatments may provide an effective therapy for metastatic breast cancer.

Materials and methods

Reagents

Emodin was purchased from Nanjing Langze Medicine and Technology Co. Ltd (Nanjing, China). Thioglycollate broth was purchased from Hi media Laboratories Pvt Ltd (Mumbai, India). Dulbecco's Modified Eagle Medium (DMEM), RPMI 1640 and fetal bovine serum (FBS) were purchased from GIBCO (Grand Island, NY). All tissue culture plastic wares were purchased from Corning (Corning, NY).

Cell culture

The 4T1 cells were cultured in RPMI 1640 containing 10% FBS, 100 U/mL penicillin (Sigma-Aldrich, St. Louis, MO) and 100 μ g/mL streptomycin (Sigma-Aldrich) at 37°C in a humidified CO₂ incubator. The EO771 cells were maintained in the same medium as described above with an addition of 2 mM glutamine (Sigma-Aldrich).

Animals

BALB/c mice (female, 6–8 weeks old) and C57BL/6 mice (female, 6–8 weeks old) were purchased from Jackson Laboratories (Bar Harbor, Maine) and housed in the University of South Carolina Animal Research Facility. Animal care procedures and experimental methods were approved by the Institutional Animal Care and Use Committee (IACUC) of the University of South Carolina according to National Institutes of Health guidelines.

4T1 cells (2×10^5) or EO771 cells (2×10^5) in 20 μ l phosphate buffered saline (PBS) were injected into both sides of the 4th pair of mammary fat pad of BALB/c or C57BL/6 mouse, respectively. The tumor size was measured using calipers every 3 days and the tumor volume was calculated using a formula: $V \text{ (mm}^3\text{)} = L \text{ (major axis)} \times W^2 \text{ (minor axis)}/2$. When the tumor volume reached 200 mm³, BALB/c or C57BL/6 mice were randomly divided into two groups. Emodin (40 mg/kg) or vehicle (2% DMSO) in 1 ml PBS was intraperitoneally injected once a day. When the animals were moribund (39 days after 4T1 cell, and 42 days after EO771 cell inoculation, respectively), the animals were sacrificed. Tumors and lungs were removed, measured and analyzed.

Histology

The lungs were perfused with PBS and fixed in 4% paraformaldehyde at room temperature (RT) for 12 h, then dehydrated in 30% sucrose at 4°C overnight, and embedded in OCT. Serial sections (8 μ m thick) were cut throughout the entire lungs. For hematoxylin and eosin (H & E) staining, sections were stained following standard procedures. Primary breast tumors were removed, fixed in 4% paraformaldehyde at RT overnight and then embedded in OCT. They were then cut into 5 μ m-thick serial sections. H & E staining was performed.

For F4/80 staining, frozen tissue sections were incubated with FITC-conjugated rat anti-F4/80 antibody (1:50, eBioscience, San Diego, CA) overnight at 4°C. For Ym1 staining, sections were first incubated with anti-mouse Ym1 rabbit polyclonal antibody (1:50, StemCell Technologies, Vancouver, BC) for 1 h at RT, and then incubated with Alexa Fluor 488-conjugated secondary antibody (1:125, Invitrogen, Grand Island, NY) for 1 h at RT. Slides were mounted with ProLong Gold Mounting Medium containing DAPI (Invitrogen), and the tissue sections were visualized using a Nikon ECLIPSE E600 microscope (Nikon Inc. Melville, NY).

For Mac2 and YM1 co-staining, frozen sections were incubated in rat anti-Mac-2 (1:50, eBioscience, San Diego, CA) and rabbit anti-mouse YM1 rabbit polyclonal antibody for 1 h at room temperature. Next the sections were incubated in FITC goat anti-rat (1:100, Invitrogen) and Alexa Fluor 555 goat anti-rabbit for 1 h at room temperature. For Mac2 and C/EBP β co-staining, frozen sections were incubated in rat anti-Mac2 (1:50) and rabbit anti-C/EBP β rabbit polyclonal antibody (1:50, Santa Cruz Biotechnology) for 1 h at room temperature. Next the sections were incubated in FITC goat anti-rat (1:100) and Alexa Fluor 555 goat anti-rabbit for 1 h at room temperature. Slides were stained with DAPI then imaged using a Zeiss LSM 510 Confocal microscope. For quantitative analysis the number of positive cells was manually counted in six random fields of view per section.

Conditioned medium collection

4T1 or EO771 cells were seeded at 5×10^6 cells per dish of 75 cm² and cultured till 90% confluence. The media were then replaced with serum-free RPMI 1640. After 24 h, the supernatants were collected and filtered through a 0.22 μ m filter.

In vitro macrophage treatment

Mice were injected with 3 ml of 3% thioglycollate intraperitoneally. Three days later, peritoneal macrophages were harvested by lavaging the peritoneal cavity with PBS and resuspended with DMEM containing 10% FBS. The non-adherent cells were removed by PBS two hours later, and the adhered macrophages were further cultured in serum-free DMEM overnight and then treated with serum-free medium, TCM or IL-4 (5 ng/ml, AASN BioAbChem Inc. Ladson, SC) with or without Emodin.

Transwell migration assay

Macrophages or tumor cells (2×10^5 cells) were seeded onto the top chamber of transwell inserts with 8 μ m pores (Corning). The inserts were then placed into 24-well plates that contained 600 μ l of serum-free RPMI 1640, 4T1 or EO771 conditioned medium alone or plus Emodin for 6 h. Cells that migrated across the inserts were stained with DAPI and counted under a fluorescence microscope at 40 \times magnification (twenty fields per well, triplicate for each group).

Quantitative Real-time PCR (qPCR)

Total RNA extraction, cDNA synthesis and qPCR were performed as described previously [11]. Primers used in qPCR are: 18s RNA, 5' CGCGGTTCTATTTTGTGGT 3' (Forward) and 5' AGTCGGCATCGTTTATGGTC 3' (Reverse); mouse Arginase 1, 5'

TTTTTCCAGCAGACCAGCTT 3' (Forward) and 5' GGAACCCAGAGAGAGCATGA 3' (Reverse). PCR thermal cycling conditions contained 3 min at 95 °C, and 40 cycles of 15 s at 95 °C and 58 s at 60 °C. Samples were run in triplicate.

Western blot

Cells were lysed in RIPA buffer (Pierce, Rockford, IL) supplemented with protease inhibitor cocktail and phosphatase inhibitors (Sigma). Total proteins were separated in 10% SDS-PAGE pre-cast gels (Bio-Rad) and transferred onto Nitrocellulose membranes (Millipore Corp., Bedford, MA). Membranes were first probed with Arginase 1 (Arg1) (1:500, BD Biosciences, San Jose, CA), Ym1 (1:500, StemCell Technologies, Vancouver, British Columbia, Canada), STAT6 (1:1000, Cell Signaling, Danvers, MA), phosphor-STAT6 (1:1000, Cell Signaling), C/EBP β (1:1000, Santa Cruz Biotechnology, Inc. Santa Cruz, CA), or β -actin (1:1000, Sigma) antibodies, followed by goat anti-rabbit secondary antibody conjugated with HRP (1:5000, Millipore Corporation, Billerica, MA) or goat anti-mouse secondary antibody conjugated with HRP (1:3000, Millipore Corporation). The Protein detection was performed using Pierce ECL Western Blotting Substrate (Pierce).

Statistical analyses

Data were presented as mean \pm standard error of the mean (SEM). Statistical significance was calculated by Student's *t* test (two-group comparison) or one-way analysis of variance (ANOVA) (multi-group comparison) using the GraphPad Prism statistical program (GraphPad Software, Inc., San Diego, CA). $p < 0.05$ was considered significant.

Results

Emodin suppressed pulmonary metastasis of breast cancer cells

To examine if Emodin can suppress pulmonary metastasis of breast cancer cells, we established an orthotopic breast cancer mouse model by injecting 4T1 cells (2×10^5) into the 4th pair of mammary glands of BALB/c mice (18 mice). After the cancer cell inoculation, the tumor growth was monitored till the tumor volume reached 200 mm³ in average on day 21 post-inoculation. The mice were randomly divided in two groups with 9 mice in each (Fig. 1A). The mice were injected intraperitoneally with vehicle (2% DMSO, Control group) or Emodin (40 mg/kg, Emodin group) in 1 ml PBS once a day. The tumor growth was further followed for 18 days. We found that mice in Control and Emodin group showed a similar tumor growth rate (Fig. 1B); and at the end-point, the tumor size and weight showed no difference between the two groups (Fig. 1C). However, Emodin significantly suppressed 4T1 lung metastatic colonization in BALB/c mice (Fig. 1D and E). There were average 11.2 ± 2.1 lung nodules formed in vehicle-treated mice, whereas Emodin treatment resulted in a 2.1-fold decrease (Fig. 1E). Moreover, the metastatic area in control group was $17.1 \pm 3.6\%$, whereas only $6.5 \pm 2.2\%$ in Emodin group (Fig. 1F).

We performed a similar experiment using another orthotopic breast cancer mouse model with inoculation of EO771 cells into C57BL/6 mice. Twenty mice were each injected with 2×10^5 EO771 cells. On day 18 post-inoculation, the average tumor volume reached 200 mm³, the mice were randomly divided into two groups, and the treatment was initiated as in

the 4T1 model and lasted for 24 days (Fig. 2A). As observed in the 4T1 model, Emodin treatment did not alter the growth of primary tumor (Fig. 2B, 2C); however, Emodin treatment significantly reduced cancer lung metastasis (Fig. 2D–F).

Emodin did not cause cytotoxicity to breast cancer cells or alter their migration at concentration achieved *in vivo*

Our previous study showed that using the 40 mg/kg i.p. administration, plasma concentration of Emodin and its biologically active metabolites reached 30 μM at 1 h and declined to 5 μM at 8 h; and at 24 h, the plasma concentration dropped below 1 μM [26]. Considering that Emodin did not affect primary tumor growth, we set to examine if Emodin at varied concentration causes cytotoxicity to breast cancer cells. As shown in Supplementary Fig. S1A, at up to 100 μM concentration, Emodin did not result in obvious toxicity to either cell types, indicating that the inhibitory effects of Emodin on breast cancer pulmonary metastasis in our models were unlikely due to its direct tumoricidal activity. To examine if Emodin directly affects breast cancer cell migration, we performed transwell assays. As shown in Fig. S1B, Emodin up to 50 μM did not reduce either 4T1 or EO771 cell migration; however, at 100 μM , Emodin significantly suppressed the migration of 4T1 cells.

Emodin reduced the accumulation of total and M2 macrophages in the lungs

Macrophages are the most prominent component of the leukocytes infiltrating within primary tumors and metastatic sites in tumor-bearing mice and humans with different types of cancers [5, 8]. Considering the robust effects of Emodin on metastasis, we hypothesize that Emodin may inhibit lung metastasis by acting on macrophages. To this end, we examined if Emodin had an impact on mobilization of macrophages into primary tumors or metastatic sites. Interestingly, the infiltration of F4/80+ macrophage in primary tumors showed no difference between Control and Emodin groups (Supplementary Fig. S2A). As opposed to classically activated or M1 macrophages that exhibit anti-tumor functions, most TAMs are alternatively activated (M2) and promote tumor development [5, 7, 8, 27]. Similar to F4/80+ macrophages, Emodin treatment resulted in little difference of Ym1+ M2 macrophage infiltration in primary tumors (Supplementary Fig. S2B). However, Emodin decreased the infiltration of F4/80+ macrophages in metastatic lungs by 3.4 folds compared to the Control group in BALB/c mice carrying 4T1 breast cancer (Fig. 3A). Similarly, Emodin decreased the infiltration of F4/80+ macrophages by 1.7 folds in C57BL/6 mice bearing EO771 cells (Fig. 3C). Next, we sought to determine if Emodin reduced M2 macrophage accumulation in metastatic lungs; and we found Emodin-treated BALB/c mice contained significantly fewer Ym1+ macrophages in the lungs than Control group (Fig. 3B). Suppression of Ym1+ macrophage accumulation in lungs by Emodin was further confirmed in EO771 breast cancer model (Fig. 3D). We also noticed that macrophages were distributed in the entire lungs, rather than being strictly associated with metastatic tumors. We further co-stained Mac2 (another pan-macrophage marker) and YM1 in the lung slides from 4T1 tumor-bearing mice. We found that in control group, 80 \pm 3% of Mac2 positive cells were also YM1 positive, while in Emodin group, 69 \pm 4% of Mac2 positive cells were also YM1 positive (Supplementary Fig. S2C), indicating that the majority macrophages in the lungs of breast cancer-bearing mice are M2 macrophages and that Emodin treatment significantly reduced the percentage of M2 type macrophages out of total lung infiltrating macrophages.

Emodin inhibited macrophage migration toward tumor conditioned medium

Accumulating evidences have demonstrated that tumor cell-secreted factors mobilize and recruit bone marrow-derived cells, including macrophages into primary tumors or metastatic sites. In light of the decreased infiltration of macrophages in lung of tumor-bearing mice treated with Emodin, we postulate that Emodin may inhibit the migration of macrophages under the influence of tumor-secreted factors. To test this, *in vitro* transwell migration assays were performed. We found that, while 4T1 cell conditioned medium (4T1 CM) induced a sharp increase of macrophage migration, Emodin significantly inhibited that in a dose-dependent manner (Fig. 4A and B). Similar phenomenon was observed when EO771 cell conditioned medium (EO771 CM) was used (Fig. 4C and D). In addition, Emodin did not affect macrophage viability at a concentration up to 100 μ M (Supplementary Fig. S3).

Emodin suppressed macrophage M2 polarization

It is well-established that tumor cell-secreted factors promote macrophage M2 polarization. Thus, we investigated if Emodin inhibits TCM-induced macrophage M2 polarization. Macrophages were stimulated with IL-4 (a potent inducer of M2 macrophage) or TCM with or without Emodin for 6 h, and then the expression of Arg1 (a marker for M2 macrophages) was determined by qPCR. We found that IL-4 induced a robust increase of Arg1 expression, whereas Emodin dose-dependently suppressed that (Fig. 5A). Similarly, Emodin significantly inhibited Arg1 expression induced by 4T1 or EO771 conditioned medium (Fig. 5A). These data indicated that Emodin inhibited macrophage M2 polarization induced by IL-4 or breast cancer cell secreted factors. Furthermore, we determined the protein levels of Arg1 and Ym1 (another marker of M2 macrophages) by western blot and found that Emodin apparently repressed the expression of Arg1 and Ym1 induced by both IL-4 and 4T1 or EO771 conditioned medium in a dose-dependent manner at either 30 min or 24 h, or both time points (Fig. 5B and C).

Emodin inhibited STAT6 and C/EBP β signaling pathways in macrophages

We next sought to investigate the molecular mechanisms by which Emodin inhibited macrophage M2 polarization. Signal transducer and activator of transcription 6 (STAT6) and CCAAT/enhancer-binding protein- β (C/EBP β) signaling pathways play critical roles in the M2 polarization of macrophages [28]. We detected the protein levels of phosphorylated STAT6 (p-STAT6) and C/EBP β in macrophages from BALB/c mice treated with IL-4 or 4T1CM with or without Emodin. As shown in Fig. 6A, IL-4 significantly increased the p-STAT6 level while Emodin dramatically reduced its expression in a dose-dependent manner. Interestingly, C/EBP β expression showed a slight increase upon IL-4 treatment, and Emodin had less inhibition on its expression. Contrast to IL-4, 4T1CM induced a dramatic increase of C/EBP β expression, especially at 24 h time point, which was significantly attenuated by Emodin. Compared to the remarkable increase of p-STAT6 by IL-4, 4T1CM caused an only slight increase of STAT6 phosphorylation. Similar to 4T1CM, EO771CM markedly increased C/EBP β level, especially at 24 h of treatment, whereas Emodin dose-dependently diminished its upregulation. EO771CM dramatically enhanced p-STAT6 level at 30 min of treatment and Emodin dose-dependently diminished the increases (Fig. 6B). To confirm if Emodin reduces C/EBP β expression in breast cancer-bearing mice, we immune-

stained C/EBP β in lung tissue slides of the mice from the 4T1 study. Confocal microscopic images showed that Emodin treatment significantly reduced C/EBP β expression in macrophages (Mac2 positive cells) in the lungs.

Discussion

Emodin has been reported to exert anticancer activities on breast cancer, prostate cancer, lung cancer, and hepatocellular carcinoma [21, 29–32], both *in vivo* and *in vitro* through inducing cell cycle arrest and apoptosis [24, 32], inhibiting angiogenesis [25], or repressing tumor cell growth, migration, and invasion [21, 33, 34]. In this current study, for the first time, we demonstrate that Emodin remarkably suppresses breast cancer lung metastasis through inhibiting the recruitment and M2 polarization of macrophages in metastatic lungs. Therefore, our study suggests that Emodin may act as a regulator of tumor microenvironment in metastatic sites through affecting macrophage biology, and thus provides new mechanistic insights into the anti-tumor function of Emodin.

Metastasis accounts for over 90% of death in cancer patients, because metastases are refractory to current treatments such as irradiation and chemotherapy as well as the more recent targeted biological therapies. Our study was aimed to investigate if Emodin exerts inhibitory effects on breast cancer lung metastasis. Metastasis is a multistep process, and is influenced by the features of primary tumor, including tumor size, blood supply and immune cell infiltration, as well as the microenvironment in the metastatic tissues/organs. Among them, the primary tumor size is a stronger predictor and significant clinical risk factor for metastases. To diminish the impact of primary tumor size on metastasis, we initiated Emodin treatment when the primary tumor grew to a substantial size (200 mm³). Using this strategy, we found that Emodin had no effects on primary tumor growth while significantly diminished lung metastasis. We postulate that Emodin, at the time being administered, may have minor effects on the well-established tumor microenvironment which is composed of tumor cells, stromal cells and bone marrow-derived cells (BMDCs), such as macrophages. Interestingly, Emodin is not cytotoxic to breast cancer cells at concentration achieved *in vivo* (up to 30 μ M). In addition, our unpublished data indeed indicated that Emodin did not inhibit multiple chemokine expression in tumor-bearing mice. Consistently, we observed that Emodin failed to affect macrophage infiltration in primary tumors. Contrast to its lack of effects on primary tumors, Emodin dramatically suppressed lung metastasis. We did not detect any metastatic nodules when we initiated Emodin administration (data not shown), thus we speculate that the tumor-favorable pre-metastatic niche may have just begun to establish at that time, and therefore the effects of Emodin are more prominent in the lungs. One interesting observation was that macrophages were evenly distributed throughout the entire lung rather than being strictly associated with metastatic tumors, suggesting that macrophages may have arrived at the lungs prior to the metastatic tumor formation, and Emodin may have started to exert its effects on metastatic lung microenvironment prior to the arrival of tumor cells.

Tumor-associated macrophages (TAMs), as the most abundant immune cell types in primary and metastatic tumors, promote tumor progression and metastasis by suppressing immune responses, increasing angiogenesis, and promoting tumor cell migration and invasion [5, 9].

It is well documented that TAMs are programmed and polarized into an immune-suppressive (M2-like) phenotype by the tumor microenvironment [5, 7, 8, 27]. Recent studies have identified a unique population of TAMs, termed metastasis-associated macrophages (MAMs) as a positive regulator for metastasis in breast cancer, bladder cancer and melanoma [11–17]. Although accumulating evidences have demonstrated that macrophages indeed play pivotal roles in metastatic sites, few studies have been conducted to investigate if MAMs are programmed and polarized into M2 macrophages. Interestingly, our recently published study demonstrated that miR155 deficient macrophages were preferentially differentiated into M2 macrophages and accumulated in metastatic lungs, resulting in enhanced lung metastasis [11]. Our current study manifested that reducing the accumulation of M2 macrophages in the lungs by Emodin dramatically inhibited pulmonary metastasis of breast cancer, presenting evidence that targeting MAM or modifying its phenotype can be of therapeutic value for metastatic cancers.

Transcriptional control of macrophage activation and differentiation is currently a subject of intense investigation. NF- κ B, hypoxia inducible factors (HIFs), signal transducer and activator of transcription (STAT), and C/EBP β are the best-known regulators for TAM activation [28, 35]. IL-4 is a prototypical direct inducer of M2 macrophage via signaling through phosphorylated STAT6 (p-STAT6), which leads to the transcriptional activation of a number of genes responsible for M2 programming [36]. Emodin markedly diminished phosphorylation of STAT6 upon IL-4 stimulation, indicating Emodin as a potent inhibitor for M2 macrophage activation. Tumor microenvironment is composed of tumor cells, stromal cells and their secreted inflammatory factors, including IL-4. Several recent studies showed that tumor cell conditioned medium can mimic the tumor microenvironment and induce *in vitro* the formation of tumor-promoting macrophages with phenotypic features similar to those of macrophages isolated from solid tumors [11, 37–39]. Reprogramming of macrophages by TCM was found primarily controlled by C/EBP β in tumors [11, 39]. Consistently, our data showed that 4T1 and EO117 TCM induced a dramatic elevation of C/EBP β expression in macrophages, while having only marginal effect on STAT6 phosphorylation. Importantly, we found Emodin significantly diminished the upregulation of C/EBP β by TCM. In light of the potent inhibitory effects of Emodin on pSTAT6 and C/EBP β , which are activated by different cytokines/chemokines secreted by tumor cells, it is conceivable that Emodin suppressed macrophage M2 polarization in the lungs by inhibiting pSTAT6 and C/EBP β signaling and thus contributed to the diminished breast cancer lung metastasis. Our confocal microscopy data confirmed that in the lungs of Emodin-treated 4T1 tumor-bearing mice, C/EBP β expression was reduced in macrophages.

In conclusion, our study, for the first time, demonstrated that Emodin suppressed breast cancer lung metastasis at least partially through inhibiting macrophage recruitment to the lungs and further attenuating M2 polarization of these recruited macrophages by targeting the p-STAT6 and C/EBP β signaling pathways. Considering that Emodin may also directly target cancer cells under certain circumstances, our study provides a new insight regarding the therapeutic potential of Emodin for breast cancer, and possibly for other cancers as well.

Supplementary Material

Refer to Web version on PubMed Central for supplementary material.

Acknowledgments

Grant Support

This work was supported by grants NIH R21AT006767 and R01HL116626 (to DF).

References

1. DeSantis C, Siegel R, Bandi P, Jemal A. Breast cancer statistics, 2011. *CA Cancer J Clin.* 2011; 61:409–418. [PubMed: 21969133]
2. Doyle DM, Miller KD. Development of new targeted therapies for breast cancer. *Breast Cancer.* 2008; 15:49–56. [PubMed: 18224395]
3. Kerbel RS. Reappraising antiangiogenic therapy for breast cancer. *Breast.* 2011; 20(Suppl 3):S56–S60. [PubMed: 22015294]
4. Martin M. Understanding the value of antiangiogenic therapy in metastatic breast cancer. *Curr Opin Oncol.* 2011; 23(Suppl):S1. [PubMed: 21490479]
5. Qian BZ, Pollard JW. Macrophage diversity enhances tumor progression and metastasis. *Cell.* 2010; 141:39–51. [PubMed: 20371344]
6. Kurahara H, Shinchi H, Mataka Y, Maemura K, Noma H, Kubo F, Sakoda M, Ueno S, Natsugoe S, Takao S. Significance of M2-polarized tumor-associated macrophage in pancreatic cancer. *J Surg Res.* 2011; 167:e211–e219. [PubMed: 19765725]
7. Allavena P, Sica A, Solinas G, Porta C, Mantovani A. The inflammatory micro-environment in tumor progression: the role of tumor-associated macrophages. *Crit Rev Oncol Hematol.* 2008; 66:1–9. [PubMed: 17913510]
8. Mosser DM. The many faces of macrophage activation. *J Leukoc Biol.* 2003; 73:209–212. [PubMed: 12554797]
9. Dai F, Liu L, Che G, Yu N, Pu Q, Zhang S, Ma J, Ma L, You Z. The number and microlocalization of tumor-associated immune cells are associated with patient's survival time in non-small cell lung cancer. *BMC Cancer.* 2010; 10:220. [PubMed: 20487543]
10. Campbell MJ, Tonlaar NY, Garwood ER, Huo D, Moore DH, Khramtsov AI, Au A, Baehner F, Chen Y, Malaka DO, Lin A, Adeyanju OO, Li S, Gong C, McGrath M, Olopade OI, Esserman LJ. Proliferating macrophages associated with high grade, hormone receptor negative breast cancer and poor clinical outcome. *Breast Cancer Res Treat.* 2011; 128:703–711. [PubMed: 20842526]
11. Yu F, Jia X, Du F, Wang J, Wang Y, Ai W, Fan D. miR-155-deficient bone marrow promotes tumor metastasis. *Mol Cancer Res.* 2013; 11:923–936. [PubMed: 23666369]
12. Qian BZ, Li J, Zhang H, Kitamura T, Zhang J, Campion LR, Kaiser EA, Snyder LA, Pollard JW. CCL2 recruits inflammatory monocytes to facilitate breast-tumour metastasis. *Nature.* 2011; 475:222–225. [PubMed: 21654748]
13. Qian B, Deng Y, Im JH, Muschel RJ, Zou Y, Li J, Lang RA, Pollard JW. A distinct macrophage population mediates metastatic breast cancer cell extravasation, establishment and growth. *PLoS One.* 2009; 4:e6562. [PubMed: 19668347]
14. Chen Q, Zhang XH, Massague J. Macrophage binding to receptor VCAM-1 transmits survival signals in breast cancer cells that invade the lungs. *Cancer Cell.* 2011; 20:538–549. [PubMed: 22014578]
15. Gil-Bernabe AM, Ferjancic S, Tlalka M, Zhao L, Allen PD, Im JH, Watson K, Hill SA, Amirkhosravi A, Francis JL, Pollard JW, Ruf W, Muschel RJ. Recruitment of monocytes/macrophages by tissue factor-mediated coagulation is essential for metastatic cell survival and premetastatic niche establishment in mice. *Blood.* 2012; 119:3164–3175. [PubMed: 22327225]

16. Said N, Sanchez-Carbayo M, Smith SC, Theodorescu D. RhoGDI2 suppresses lung metastasis in mice by reducing tumor versican expression and macrophage infiltration. *J Clin Invest.* 2012; 122:1503–1518. [PubMed: 22406535]
17. Said N, Smith S, Sanchez-Carbayo M, Theodorescu D. Tumor endothelin-1 enhances metastatic colonization of the lung in mouse xenograft models of bladder cancer. *J Clin Invest.* 2010; 121:132–147. [PubMed: 21183790]
18. Shang XY, Yuan ZB. [Determination of six effective components in Rheum by cyclodextrin modified micellar electrokinetic chromatography]. *Yao Xue Xue Bao.* 2002; 37:798–801. [PubMed: 12567865]
19. Xia XM, Li BK, Xing SM, Ruan HL. Emodin promoted pancreatic claudin-5 and occludin expression in experimental acute pancreatitis rats. *World J Gastroenterol.* 2012; 18:2132–2139. [PubMed: 22563203]
20. Zhou M, Xu H, Pan L, Wen J, Guo Y, Chen K. Emodin promotes atherosclerotic plaque stability in fat-fed apolipoprotein E-deficient mice. *Tohoku J Exp Med.* 2008; 215:61–69. [PubMed: 18509236]
21. Liu A, Chen H, Wei W, Ye S, Liao W, Gong J, Jiang Z, Wang L, Lin S. Antiproliferative and antimetastatic effects of emodin on human pancreatic cancer. *Oncol Rep.* 2011; 26:81–89. [PubMed: 21491088]
22. Shrimali D, Shanmugam MK, Kumar AP, Zhang J, Tan BK, Ahn KS, Sethi G. Targeted abrogation of diverse signal transduction cascades by emodin for the treatment of inflammatory disorders and cancer. *Cancer Lett.* 2013; 341:139–149. [PubMed: 23962559]
23. Yanaihara N, Caplen N, Bowman E, Seike M, Kumamoto K, Yi M, Stephens RM, Okamoto A, Yokota J, Tanaka T, Calin GA, Liu CG, Croce CM, Harris CC. Unique microRNA molecular profiles in lung cancer diagnosis and prognosis. *Cancer Cell.* 2006; 9:189–198. [PubMed: 16530703]
24. Wang ZH, Chen H, Guo HC, Tong HF, Liu JX, Wei WT, Tan W, Ni ZL, Liu HB, Lin SZ. Enhanced antitumor efficacy by the combination of emodin and gemcitabine against human pancreatic cancer cells via downregulation of the expression of XIAP in vitro and in vivo. *Int J Oncol.* 2011; 39:1123–1131. [PubMed: 21743963]
25. Kaneshiro T, Morioka T, Inamine M, Kinjo T, Arakaki J, Chiba I, Sunagawa N, Suzui M, Yoshimi N. Anthraquinone derivative emodin inhibits tumor-associated angiogenesis through inhibition of extracellular signal-regulated kinase 1/2 phosphorylation. *Eur J Pharmacol.* 2006; 553:46–53. [PubMed: 17056031]
26. Jia X, Iwanowycz S, Wang J, Saaoud F, Yu F, Wang Y, Hu J, Chatterjee S, Wang Q, Fan D. Emodin attenuates systemic and liver inflammation in hyperlipidemic mice administrated with lipopolysaccharides. *Exp Biol Med (Maywood).* 2014
27. Ruffell B, Affara NI, Coussens LM. Differential macrophage programming in the tumor microenvironment. *Trends Immunol.* 2012; 33:119–126. [PubMed: 22277903]
28. Lawrence T, Natoli G. Transcriptional regulation of macrophage polarization: enabling diversity with identity. *Nat Rev Immunol.* 2011; 11:750–761. [PubMed: 22025054]
29. Yu CX, Zhang XQ, Kang LD, Zhang PJ, Chen WW, Liu WW, Liu QW, Zhang JY. Emodin induces apoptosis in human prostate cancer cell LNCaP. *Asian J Androl.* 2008; 10:625–634. [PubMed: 18478162]
30. Hsu CM, Hsu YA, Tsai Y, Shieh FK, Huang SH, Wan L, Tsai FJ. Emodin inhibits the growth of hepatoma cells: finding the common anti-cancer pathway using Huh7, Hep3B, and HepG2 cells. *Biochem Biophys Res Commun.* 2010; 392:473–478. [PubMed: 19895793]
31. He L, Bi JJ, Guo Q, Yu Y, Ye XF. Effects of emodin extracted from Chinese herbs on proliferation of non-small cell lung cancer and underlying mechanisms. *Asian Pac J Cancer Prev.* 2012; 13:1505–1510. [PubMed: 22799356]
32. Ma YS, Weng SW, Lin MW, Lu CC, Chiang JH, Yang JS, Lai KC, Lin JP, Tang NY, Lin JG, Chung JG. Antitumor effects of emodin on LS1034 human colon cancer cells in vitro and in vivo: roles of apoptotic cell death and LS1034 tumor xenografts model. *Food Chem Toxicol.* 2012; 50:1271–1278. [PubMed: 22321733]

33. Lu HF, Lai KC, Hsu SC, Lin HJ, Kuo CL, Liao CL, Yang JS, Chung JG. Involvement of matrix metalloproteinases on the inhibition of cells invasion and migration by emodin in human neuroblastoma SH-SY5Y cells. *Neurochem Res.* 2009; 34:1575–1583. [PubMed: 19291397]
34. Chen YY, Chiang SY, Lin JG, Ma YS, Liao CL, Weng SW, Lai TY, Chung JG. Emodin, aloemodin and rhein inhibit migration and invasion in human tongue cancer SCC-4 cells through the inhibition of gene expression of matrix metalloproteinase-9. *Int J Oncol.* 2010; 36:1113–1120. [PubMed: 20372784]
35. Zhou D, Huang C, Lin Z, Zhan S, Kong L, Fang C, Li J. Macrophage polarization and function with emphasis on the evolving roles of coordinated regulation of cellular signaling pathways. *Cell Signal.* 2013
36. Liu G, Yang H. Modulation of macrophage activation and programming in immunity. *J Cell Physiol.* 2012; 228:502–512. [PubMed: 22777800]
37. Liu Y, Chen K, Wang C, Gong W, Yoshimura T, Liu M, Wang JM. Cell surface receptor FPR2 promotes antitumor host defense by limiting M2 polarization of macrophages. *Cancer Res.* 2013; 73:550–560. [PubMed: 23139214]
38. Yang J, Zhang Z, Chen C, Liu Y, Si Q, Chuang TH, Li N, Gomez-Cabrero A, Reisfeld RA, Xiang R, Luo Y. MicroRNA-19a-3p inhibits breast cancer progression and metastasis by inducing macrophage polarization through downregulated expression of Fra-1 proto-oncogene. *Oncogene.* 2013
39. He M, Xu Z, Ding T, Kuang DM, Zheng L. MicroRNA-155 regulates inflammatory cytokine production in tumor-associated macrophages via targeting C/EBPbeta. *Cell Mol Immunol.* 2009; 6:343–352. [PubMed: 19887047]

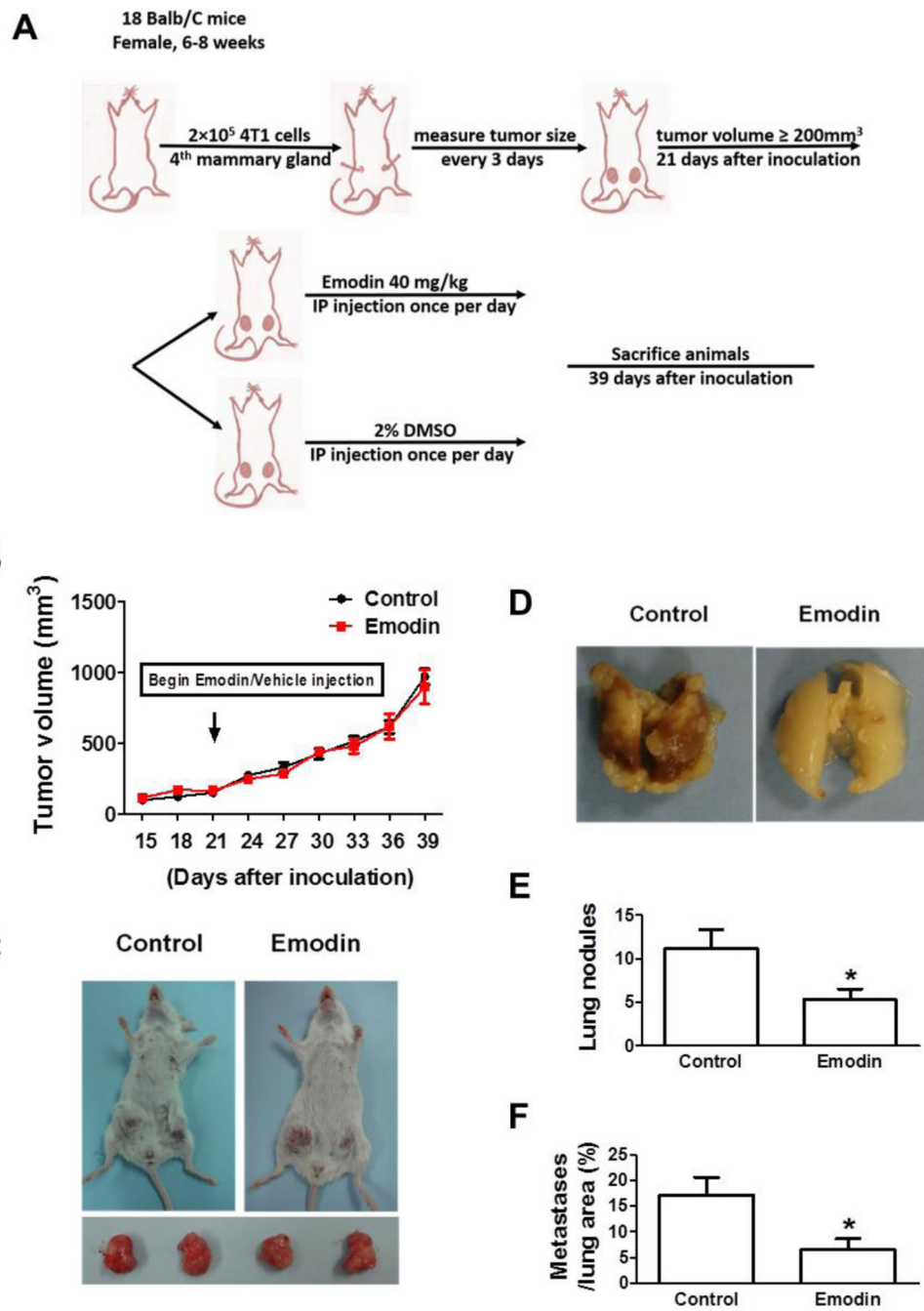


Figure 1. Emodin suppressed breast cancer lung metastasis in 4T1 orthotopic mouse model. **A.** *In vivo* experimental protocol of 4T1 cells in BALB/c mice as described in methods. **B.** Growth curve of 4T1 primary tumors in BALB/c mice. Tumor volume was shown as mm³. Each data point represents the mean ± SEM of 9 mice. **C.** Representative primary tumors in BALB/c mice. **D.** Representative gross lung images of BALB/c mice carrying 4T1 cells. **E.** Quantification of tumor nodules per lung in BALB/c mice (n=9). Data are presented as the

mean \pm SEM. F. The percentage of metastatic tumor area in whole lung sections. Data are presented as the mean \pm SEM. * p <0.05 vs Control.

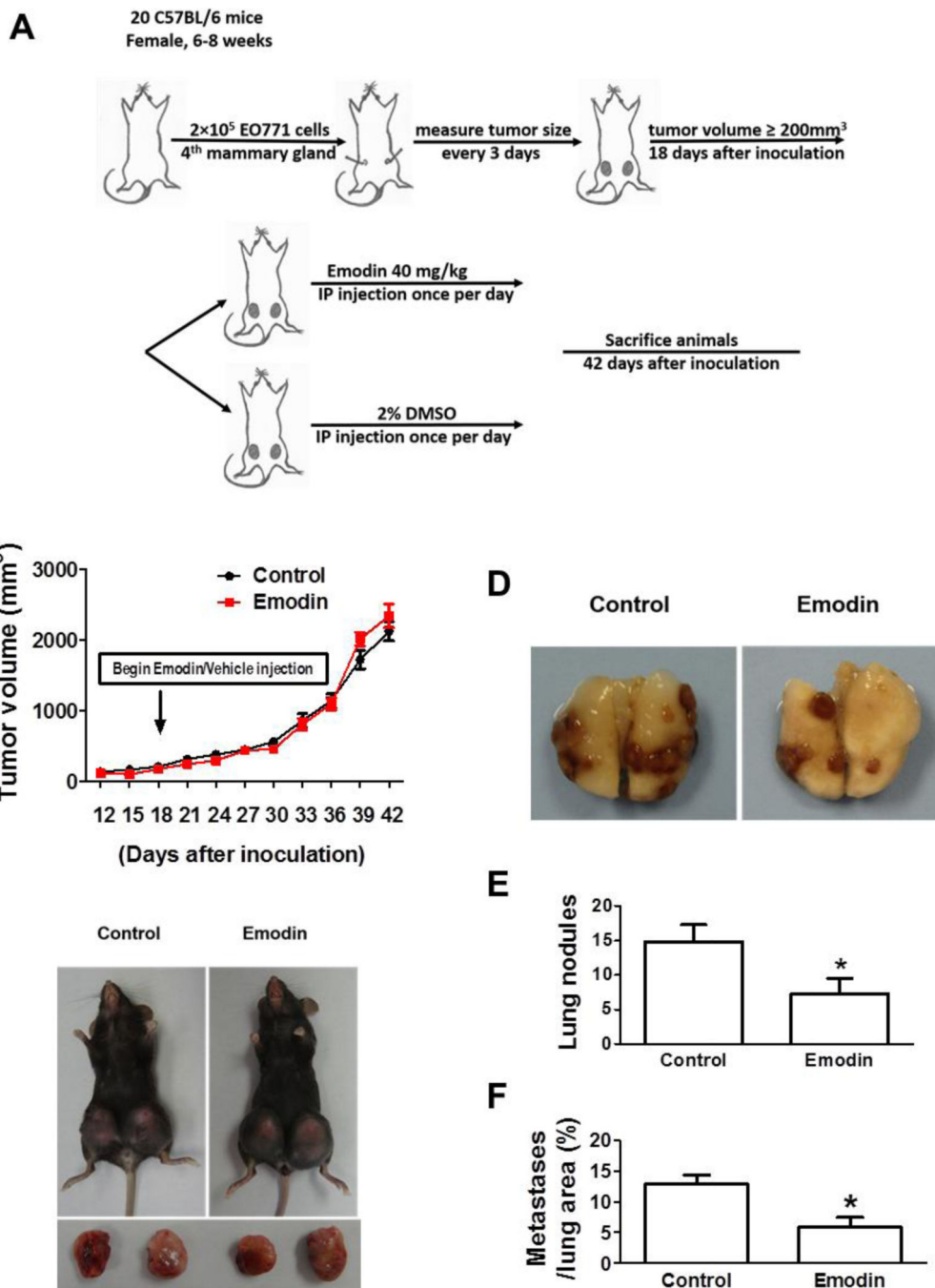


Figure 2. Emodin suppressed breast cancer lung metastasis in EO771 orthotopic mouse model. **A.** *In vivo* experimental protocol of EO771 cells in C57BL/6 mice as described in methods. **B.** Growth curve of EO771 primary tumors in C57BL/6 mice. Tumor volume was shown as mm³. Each data point represents the mean ± SEM of 10 mice. **C.** Representative primary tumors in C57BL/6 mice. **D.** Representative gross lung images of C57BL/6 mice carrying EO771 breast cancer. **E.** Quantification of tumor nodules per lung in C57BL/6 mice (n=10).

Data are presented as the mean \pm SEM. F. The percentage of metastatic tumor area in whole lung sections. Data are presented as the mean \pm SEM. * p <0.05 vs Control.

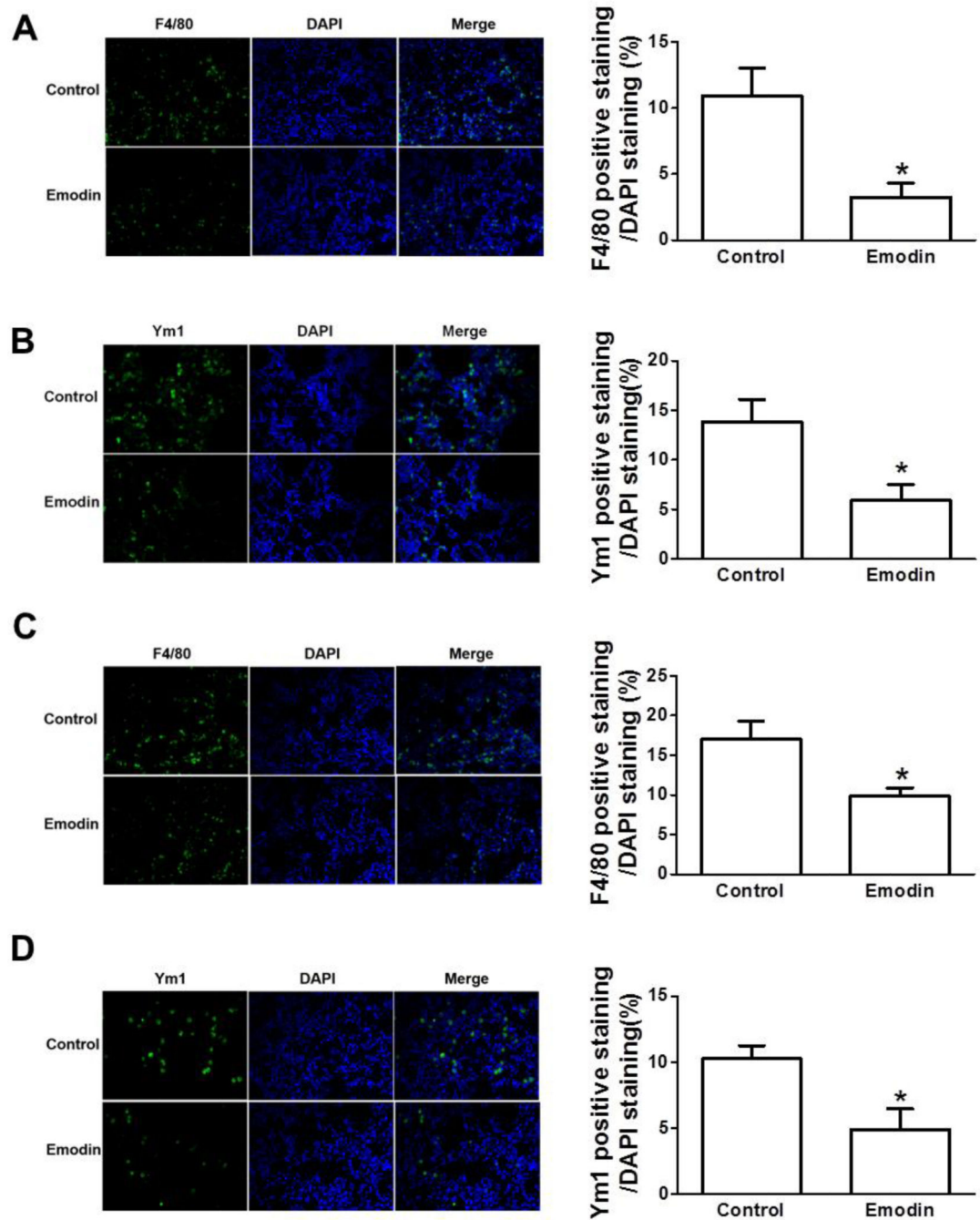


Figure 3.

Emodin reduced the numbers of F4/80+ total macrophages and Ym1+ M2 macrophages in the lungs of tumor-bearing mice. Lung sections from BALB/c mice carrying 4T1 breast cancer cells (A and B) or C57BL/6 mice carrying EO771 cells (C and D) were stained with F4/80 or Ym1 antibody to visualize total or M2 macrophages. The percentage of F4/80 or Ym1 positive cells was calculated as a ratio of green cells to DAPI+ blue cells. Ten random non-overlapping fields from sections of each mouse were examined. Data are presented as the mean \pm SEM. * $p < 0.05$. Magnification, 40 \times .

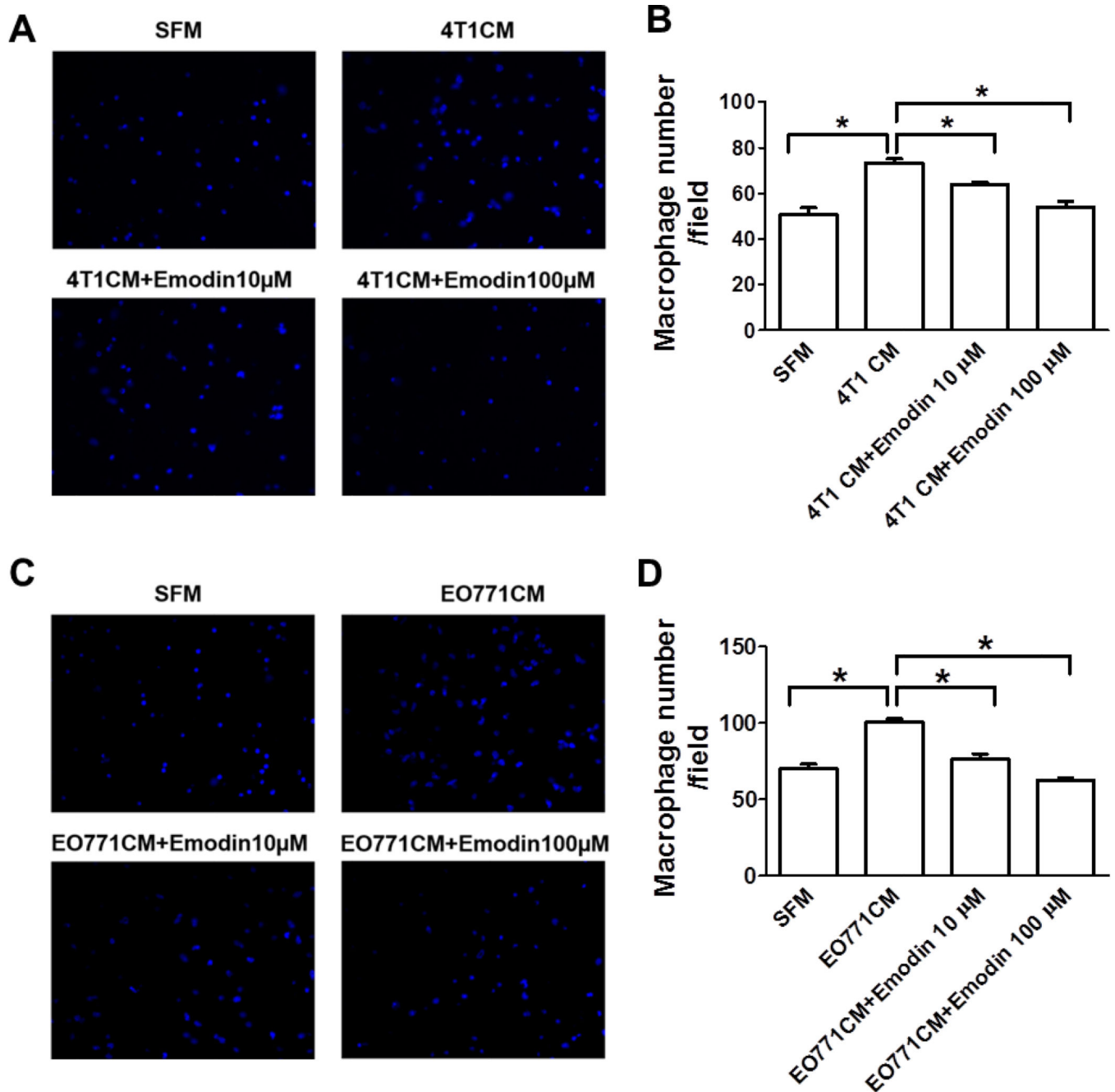


Figure 4. Emodin inhibited macrophage migration toward tumor conditioned medium. Transwell migration assays were performed to measure macrophage migration towards serum free medium (SFM) and 4T1 (A and B) or EO771 (C and D) tumor conditioned medium (4T1 CM and EO771 CM, respectively) with or without Emodin. Data were presented as the mean \pm SEM of three replicates. * p <0.05. Representative immunofluorescence images of migrated macrophages toward 4T1 CM (A) or EO771 CM (C) were shown. DAPI was used to stain the nucleus. Magnification, 40 \times .

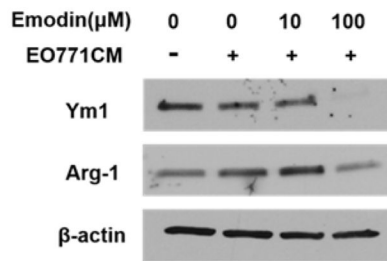
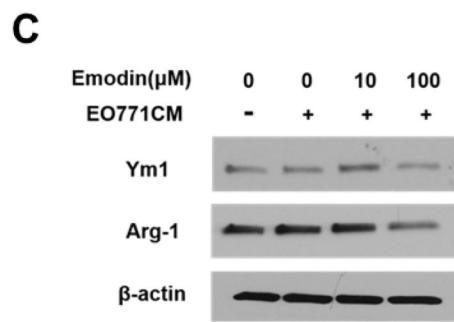
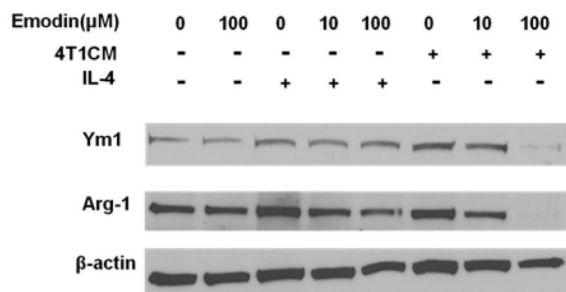
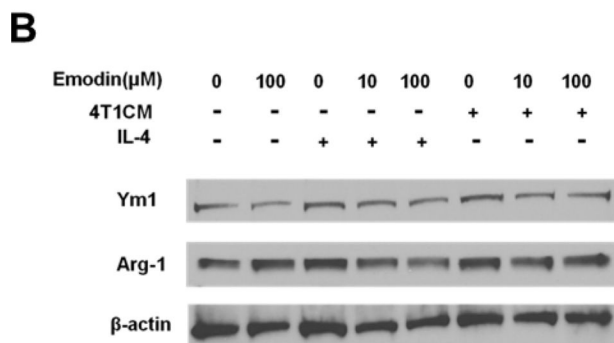
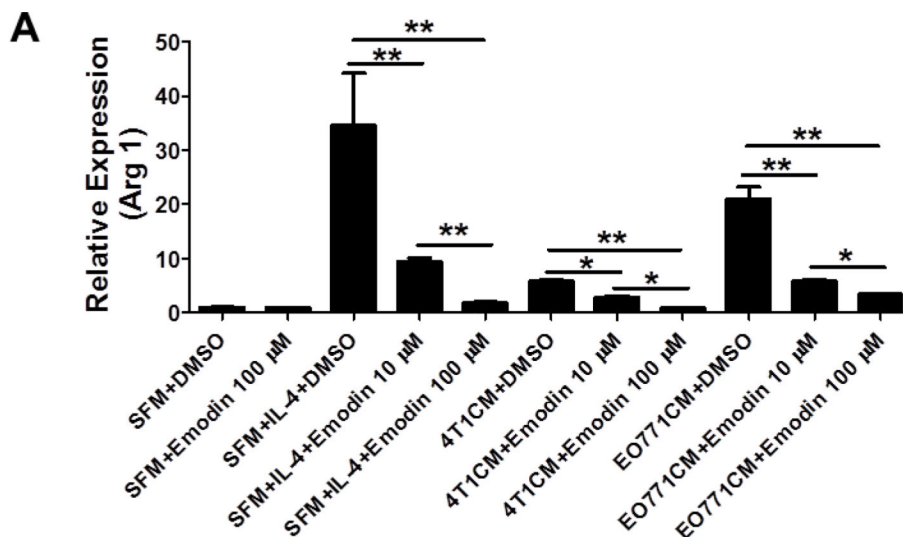


Figure 5. Emodin suppressed macrophage M2 polarization. **A.** Quantitative real-time PCR was performed to detect Arg1 mRNA levels in cultured mouse macrophages stimulated with IL-4 (5 ng/ml), 4T1 or EO771 TCM with or without Emodin (10 or 100 μM) for 6 h. Data are presented as the mean ± SEM of three replicates. * $p < 0.05$. ** $p < 0.01$. **B.** Western blot was performed to measure the expression of Arg-1 and Ym1 proteins in BALB/c peritoneal macrophages stimulated with IL-4 (5 ng/ml), 4T1 CM with or without Emodin (10 and 100 μM) for 30 min or 24 h. **C.** Western blot analysis of Arg1 and Ym1 expression in C57BL/6

mouse macrophages stimulated with EO771 CM with or without Emodin for 30 min or 24 h. β -actin is used as a loading control. SFM: serum free medium; 4T1CM: 4T1 cell conditioned medium; EO771CM: EO771 cell conditioned medium.

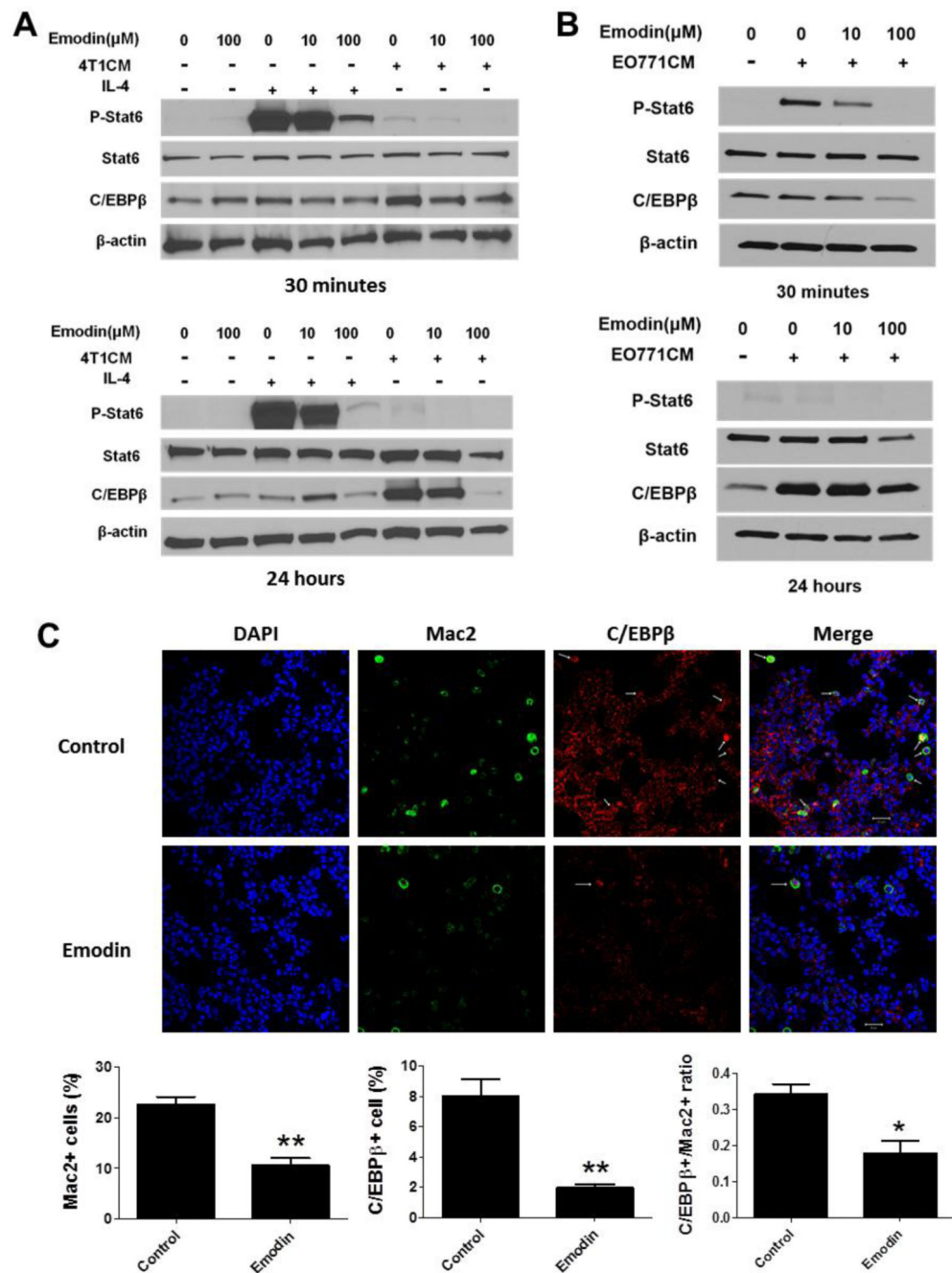


Figure 6. Emodin inhibited STAT6 and C/EBPβ signaling in macrophages. **A.** Western blot analysis of phosphorylated STAT6 (p-STAT6) and C/EBPβ expression in BALB/c mouse macrophages treated with IL-4 or 4T1 CM with or without Emodin. **B.** Western blot analysis of p-STAT6 and C/EBPβ expression in C57BL/6 mouse macrophages treated with EO771 CM with or without Emodin. β-actin was used as a loading control. Representative blots of 3–4 experiments were shown. **C.** Confocal microscopic images of lung tissue slides from 4T1 breast cancer-bearing mice. The slides were co-stained for DAPI (Blue, nucleus), Mac2

(Green, pan macrophage marker) and C/EBP β (Red). The quantitative results were shown under the images. N=5 for each group, * p <0.05; ** p <0.001, vs Control.